Journal of Asian Earth Sciences 45 (2012) 167–178

Contents lists available at SciVerse ScienceDirect

Journal of Asian Earth Sciences

journal homepage: www.elsevier.com/locate/jseaes

Tectonic implications and seismicity triggering during the 2008 Baluchistan, Pakistan earthquake sequence

R.B.S. Yadav [a,*], V.K. Gahalaut [b], Sumer Chopra [c], Bin Shan [d]

[a] Indian National Centre for Ocean Information Services (INCOIS), Hyderabad, India
[b] National Geophysical Research Institute, Hyderabad, India
[c] Seismology Division, Ministry of Earth Sciences, CGO Complex, New Delhi 110003, India
[d] Key Laboratory of Dynamical Geodesy, Institute of Geodesy and Geophysics, Chinese Academy of Science, Wuhan 430077, China

ARTICLE INFO

Article history:
Received 13 April 2011
Received in revised form 11 October 2011
Accepted 16 October 2011
Available online 25 November 2011

Keywords:
Baluchistan (Pakistan) earthquake
b-Value
Omori law
Modified Bath's law
Coulomb failure stress

ABSTRACT

A damaging and widely felt moderate earthquake (Mw 6.4) hit the rural, mountainous region of southwestern Pakistan on October 28, 2008. The main shock was followed by another earthquake of identical magnitude (Mw 6.4) on the next day. The spatial distribution of aftershocks and focal mechanism revealed a NW–SE striking rupture with right-lateral strike-slip motion which is sympathetic to the NNW–SSE striking active mapped Urghargai Fault. The occurrence of strike-slip earthquakes suggests that along with the thrust faults, strike slip faults too are present beneath the fold-and-thrust belt of Sulaiman–Kirthar ranges and accommodates some of the relative motion of the Indian and Eurasian plates.

To assess the characteristics of this sequence, the statistical parameters like aftershocks temporal decay, *b*-value of G–R relationship, partitioning of radiated seismic energy due to aftershocks, and spatial fractal dimension (D-value) have been examined. The *b*-value is estimated as 1.03 ± 0.42 and suggests the tectonic genesis of the sequence and crustal heterogeneity within rock mass. The low *p*-value of 0.89 ± 0.07 implies slow decay of aftershocks activity which is probably an evidence for low surface heat flow. A value of spatial fractal dimension of 2.08 ± 0.02 indicates random spatial distribution and that the source is a two-dimensional plane filled-up by fractures.

The static coseismic Coulomb stress changes due to the foreshock (Mw 5.3) were found to increase stress by more than 0.04 bars at the hypocenter of the main shock, thus promoting the failure. The cumulative coseismic Coulomb stress changes due to the foreshock and mainshocks suggest that most of the aftershocks occurred in the region of increased Coulomb stress, and to the SE to the mainshock rupture.

1. Introduction

A devastating earthquake of magnitude Mw 6.4 occurred on October 28, 2008 (23:09:57 GMT) near Ziarat city in the province of Baluchistan of SW Pakistan (Figs. 1 and 2) which caused a heavy loss of lives and properties in the surrounding region. The Baluchistan, along with Quetta and Sulaiman fold and thrust belt, constitutes the most active part of shallow seismicity in SW Pakistan and falls under seismic zone 4, the most severe seismic zone in the Building Code of Pakistan 2007 (BCP, 2007). The seismicity of the study area is mainly related to the ongoing transpressional collision between Indian and Eurasian plates (Fig. 1). The earthquake of October 28, 2008 is located approximately 80 km east of the 650 km long Chaman fault, which is a major left-lateral strike-slip fault in the study region and accommodates a significant amount of slip across the plate boundary of the Indian and Eurasian plates. The epicenter is located approximately 50 km northeast of the region of the most intense damage from the epicenter of the devastating Quetta earthquake of May 30, 1935 (Mw 7.6), which was estimated to have killed about 30,000–60,000 people (Maqsood and Schwarz, 2010). The focal mechanism solution obtained by Global Centroid Moment Tensor (GCMT) solution and USGS shows a right-lateral strike-slip faulting with some reverse component. The occurrence of such type of earthquakes in this region suggests that the relative motion between the India Eurasia plates is also accommodated through strike-slip motion on such faults under the Sulaiman fold-and-thrust belt. A look into the historical and modern seismicty of Pakistan (Fig. 1) reveals that the seismic hazard is more in the Baluchistan province and in particular Sulaiman fold and thrust belt region.

The earthquake parameters were estimated by local as well as international seismological agencies and listed in Table 1. The US

* Corresponding author. Tel.: +91 40 23886094; fax: +91 40 23895012.
E-mail addresses: rbsybhu@rediffmail.com, rbsyiitr@indiatimes.com (R.B.S. Yadav).

1367-9120/$ - see front matter © 2011 Elsevier Ltd. All rights reserved.
doi:10.1016/j.jseaes.2011.10.003

Geological Surveys (USGS) National Earthquake Information Centre (http://www.neic.usgs.gov) located this earthquake at lat. 30.656° N and long. 67.361° E with depth of 15 km (Table 1). However, local observatory of Water and Power Development Authority (WPDA) of Pakistan located this event at lat. 30.660° N and long. 67.440° E at a distance of 51 km from Ziarat and 60 km NE from Quetta (Lisa and Jan, 2010). After 12 h of the occurrence of main shock, another earthquake of identical magnitude (Mw 6.4) occurred about 20 km SE of the main shock epicenter. We have considered this event as the doublet of the main shock due to the similar focal mechanism, focal depth and identical size (Table 2), as also considered by Lisa and Jan (2010), but the characteristics of this event should be assessed in detail to confirm it as a doublet of the main shock. Therefore, we have not considered it as a second largest aftershock of this sequence. The main shock was preceded by a moderate size foreshock of magnitude Mw 5.3 occurred about 20 km SE of the main shock epicenter (shown by square in Fig. 2) that caused some damage in the epicentral region. Shaking due to this seismic sequence was felt in most part of the Baluchistan region. The intensity of the main shock was VIII on modified Mercalli Intensity (MMI) scale in and around the Ziarat region (PMD report, 2009). This seismic sequence claimed about 164 lives, 173 injured and more than 120,000 people were affected due to this earthquake (Maqsood and Schwarz, 2010). More than 5000 buildings were destroyed and another about 4000 were damaged in the Baluchistan province and surrounding regions (Maqsood and Schwarz, 2010). The main shock was strongly felt in the districts of Ziarat and Pishni but causalities were also reported from Chaman and Dera Jamali areas. Several villages were affected due to landslides in the Ziarat area.

The purpose of present study is to investigate in detail the properties of the aftershock sequence of this earthquake using well-established statistical models of aftershocks. For this purpose, a statistical assessment of aftershocks data was performed (*b*-value, *p*-value, *D*-value, and partitioning of radiated seismic energy) to shed light on the seismotectonic properties of the study area. In addition, an attempt has been made to assess future seismic hazard by examining the static Coulomb stress field due to coseismic slip of foreshock and mainshocks for the identification of the possible regions of aftershocks activity.

2. Tectonic set-up and seismicity of study region

The tectonics of Baluchistan and adjoining regions is very complex and peculiar in nature. The interaction of northward moving Indian plate with the Afghan block and Eurasian plate since Cretaceous is responsible for the major tectonic features in the Baluchistan region. The tectonics and structural style of this region is mainly controlled by various tectonic elements like southward progressing Sulaiman Lobe, Chaman Transform Fault and resistant mass at Sibi. Direct collision in northern Pakistan results in transpression along the Chaman fault (Lawrence et al., 1981; Farah et al., 1984). The oblique convergence along the Chaman fault boundary is responsible for the lobate Sulaiman fold belt towards southeast of the Chaman fault. The Afghan block to the northwest of Chaman fault consists of microfragments that were drifted from Gondwanaland and accreted to the Eurasian landmass during late Paleozoic through Cenozoic times (Bordet, 1978; Boulin, 1981; Tapponnier et al., 1981). The Sulaiman fold-thrust belt is located along a zone of transpression in the northwestern part of the

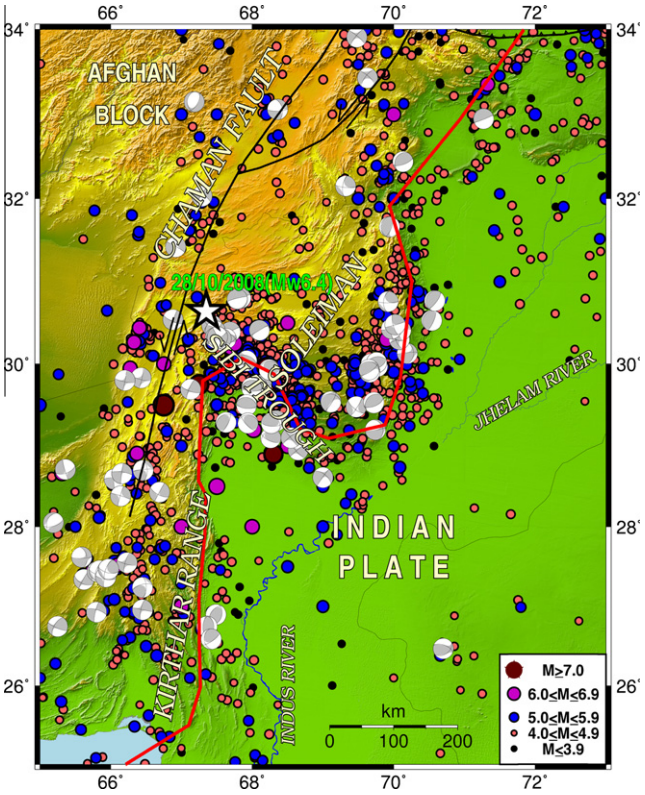

Fig. 1. Seismotectonic map of Pakistan and adjoining region showing the major structural features and seismic activity from 1852 to March 2009. Seismic events are shown with circles. Major faults are shown with thick line. Star shows the epicenter of Baluchistan earthquake of magnitude Mw 6.4 occurred on October 28, 2008. Maximum seismic activity in Baluchistan region is observed towards SE of this earthquake. The focal mechanism solutions of earthquakes obtained by GCMT catalog during 1976–2008 are shown with gray color beach ball.

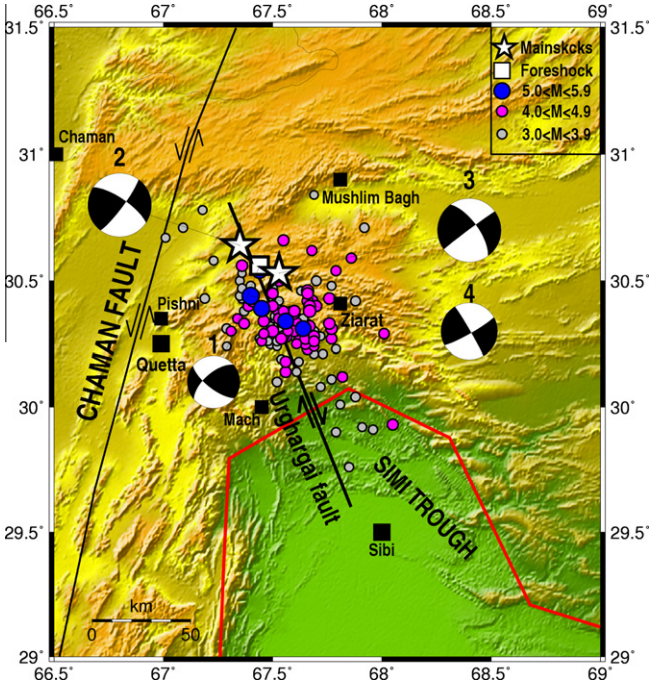

Fig. 2. Epicentral location of Baluchistan earthquake sequence (foreshock, mainshocks doublet and aftershocks) occurred during the period of October 28–December 31, 2008. Mainshocks doublet (Mw 6.4) are shown by stars and foreshock (Mw 5.3) is shown by open square. Focal mechanism solutions of the four largest earthquakes of this sequence (listed in Table 2) are plotted as lower hemisphere equal area projection. Number at the top of beach ball indicates the serial no. of that event listed in Table 2. The active right-lateral strike-slip Urghargai fault identified by Kazmi (1979) is shown by solid line striking NNW–SSE direction, which strike is in accordance with the strike of aftershocks activity and may be causative fault of this sequence.

Table 1
Source parameters of October 28, 2008 Baluchistan main shock determined by different local and international seismological agencies.

S.no.	Date (YYYY.MO.DA)	Time (HH MM SS.S)	Lat. (°N)	Long. (°E)	Depth (km)	Magnitude (Mw)	Source
1	2008.10.28	23 10 02.0	30.656	67.361	15	6.4	NEIC, USGS
2	2008.10.28	23 10 02.0	30.400	67.480	17.2	6.4	GCMT
3	2008.10.28	23 10 00.7	30.580	67.410	41	6.6	GEOFON
4	2008.10.28	23 09 57.4	30.700	67.360	10	6.4	EMSC
6	2008.10.28	23 09 59.1	30.660	67.440	10	6.4	WAPDA
7	2008.10.28	23 10 00.0	30.612	67.436	15	6.5 (m_b)	PMD

NEIC, USGS: National Earthquake Information Centre (NEIC) of US Geological Survey (USGS), GCMT: Global Centroid Moment Tensor, GEOFON: GFZ seismic network, EMSC: European Mediterranean Seismological Centre, WAPDA: Water and Power Development Authority of Pakistan, PMD: Pakistan Meteorological Department.

Table 2
Seismic parameters and focal mechanism solutions of four largest earthquakes in Baluchistan earthquake sequence. The centroid depth, moment magnitude (Mw) and focal mechanism solutions have been taken from Global Centroid Moment Tensor (GCMT) catalog, whereas other parameters have been taken from NEIC of USGS.

S.no.	Date (YYYY.MO.DA)	Time (HH MM SS.S)	Lat. (°N)	Long (°E)	Depth (km)	Magnitude (Mw)	Focal mechanism solution		
							Strike	Dip	Rake
1	2008.10.28	22 33 12.9	30.560	67.440	16.6	5.3	128	70	151
2	2008.10.28	23 10 02.0	30.656	67.361	17.2	6.4	304	73	171
3	2008.10.29	11 32 48.6	30.600	67.460	12.0	6.4	324	68	−178
4	2008.12.09	22 52 40.0	30.440	67.400	12.0	5.7	330	87	173

Indian subcontinent. The most prominent geodynamic feature of Pakistan is left-lateral strike-slip Chaman fault that separates Indian and Eurasian plate.

The seismic activity in Baluchistan, Pakistan region is mainly related with the ongoing continent–continent collision of Indian and Eurasian plates. The entire Baluchistan region is characterized by shallow depth seismicity, generally less than 50 km depth. The seismicity pattern shows a distinct relationship with tectonic features associated with the region (Rowlands, 1978; Ambraseys and Bilham, 2003). The focal-mechanism of earthquakes suggests that Baluchistan arc is a major left-lateral shear zone, located between the Afghan block and the Indian shield (Verma et al., 1980). Transcurrent faulting takes place along north–south directed faults within the Sulaiman–Kirthar ranges whereas Sulaiman wrench zone is the most active part of the Baluchistan arc affected by lateral faulting. The Baluchistan region of Pakistan has been devastated by several large earthquakes in the past (Fig. 1) which caused heavy damage in the region. Ambraseys and Bilham (2003) documented the most reliable seismic history of this region. Yadav (2009) assessed the spatio-temporal properties of four largest earthquakes ($M \geqslant 7.0$) occurred in this region and observed that there is a spatial migration of such earthquakes in this region from northeast to southwest direction. In addition to the large damaging earthquakes, the Baluchistan region has also experienced a number of moderate earthquakes in the past which caused some destruction of lives and properties in the region (Fig. 1).

3. The 28 October 2008 Baluchistan earthquake and its aftershocks sequence

The Baluchistan earthquake sequence (foreshock, main shock doublet and aftershocks) consists of more than 1185 earthquakes of M_L 2.2–4.8 recorded by Pakistan Meteorological Department (PMD) till January 30, 2009 with the help of at least four portable seismometers installed in the epicentral region (PMD report, 2009). PMD reported more than 200 aftershocks of magnitude $M \geqslant 4.0$ within this period. The National Earthquake Information Centre (NEIC) of US Geological Survey (USGS) reported 126 events of magnitude $m_b \geqslant 3.0$ during the period October 28 to December 31, 2008 consisting of about 66 events (52%) with magnitude $m_b \geqslant 4.0$. The occurrence of larger magnitude aftershocks in this sequence reveals that large size asperities exist in the rupture zone of main shock from where seismic energy released in the form of moderate size aftershocks. The Baluchistan earthquake sequence started with a moderate size foreshock of magnitude Mw 5.3 occurred about 40 min before the occurrence of main shock at a distance of 20 km southeast of the main shock epicenter. The fault plane solution determined by Global Centroid Moment Tensor (GCMT) solutions (http://www.globalcmt.org/CMTsearch.html) shows that foreshock occurred either on a NE–SW oriented plane with predominantly left-lateral motion or on a NW–SE oriented plane with right lateral motion with some reverse component. This foreshock was followed by a main shock of magnitude Mw 6.4 in the early morning of October 29, 2008 at a local time of 05:10 PST at about 60 km northeast of the Quetta city. The earthquake was felt in most part of Baluchistan region including some adjacent part of Sindh province. The earthquake exhibited a similar motion as in case of the foreshock (Fig. 2, Table 2). Lisa and Jan (2010) determined fault plate solution for this earthquake using first motion data from PMD and WAPDA seismic stations. Their estimation also shows a similar fault plane solution for this earthquake. The NW–SE oriented right-lateral strike slip faults are typical in the Baluchistan region. A steep dip (73°) for main shock fault rupture is rare in this region and is much steeper than normally found in the Sulaiman range (Lisa and Jan, 2010). The Baluchistan region mainly consists of reverse/thrust faults along with some strike slip. Kazmi (1979) mapped an active right-lateral strike-slip fault striking in NNW–SSE direction known as Urghargai fault (Fig. 2) in this region with the help of satellite images and field studies which might be extending down to a depth of about 10–15 km. The location and fault plane solution of the main shock indicate that Urghargai fault was probably the causative fault for this earthquake.

The spatial distribution of aftershocks activity of magnitude $m_b \geqslant 3.0$ occurred during this seismic sequence for the period October 28 to December 31, 2008 and located by NEIC of USGS shows NW–NNW trend (Fig. 2). The CMT solutions determined by Columbia University (http://www.ldeo.columbia.edu/research/seismology-geology-tectonophysics/global-cmt) for four stronger earthquakes in the sequence (foreshock, main shock doublet and largest aftershock) are listed in Table 2 and shown in Fig. 2 along with the epicenters of foreshock and aftershocks. Most of the aftershocks are clustered in the NW to NNW direction coinciding with the strike of one of the nodal plane (strike = 304°, dip = 73°, rake = 171°) of the main shock's fault plane solution and in good

agreement with the active right-lateral Urghargai Fault striking NNW–SSE direction identified by Kazmi (1979) in this region. Majority of the aftershocks of this sequence occurred to the SE of the main shock epicenter suggesting that the main rupture propagated towards SE. Lisa and Jan (2010) assigned intensity VIII (MMI scale) on the basis of information obtained from print and electronic media. A number of landslides triggered due to this earthquake in the surrounding region of Ziarat that caused some damages in the region. The intensity map prepared by Lisa and Jan (2010) based on damage scenario shows also NW–SE directed isoseismals corresponding with the overall trend of epicenters of aftershocks.

4. Statistical properties of the aftershock sequence

The characteristics of a seismic sequence in space, time, and size have been described by a number of statistical models by various researchers in the world (Utsu, 1961; Bath, 1965; Ranalli, 1969; Papazachos, 1971; Shcherbakov and Turcotte, 2004; Yadav et al., 2011). The main characteristics commonly studied in seismic sequences are the frequency–magnitude distribution described by the Gutenberg–Richter relation, the decay rate of aftershocks following the modified Omori law and fractal dimension. The studies of statistical properties of occurrence of the aftershocks have been one of the main objectives of the seismological studies in connection with the processes of earthquake generation. In the following subsections, we investigate the physical properties of the Baluchistan earthquake sequence on the basis of commonly accepted and widely applied empirical and statistical laws. For this purpose, the aftershocks data reported by NEIC of US Geological Survey during the period October 28, 2008–December 31, 2008 of magnitude $m_b \geqslant 3.0$ have been considered due to non-availability of more complete and reliable data from local sources.

4.1. Frequency–magnitude scaling relationship

The frequency–magnitude scaling statistics for earthquakes, a type of power law size distribution, is well approximated by G–R relation (Gutenberg and Richter, 1944) that was first introduced by Ishimoto and Iida (1939)

$$\log_{10} N(\geqslant M) = a - bM \tag{1}$$

where $N(\geqslant M)$ is the cumulative number of earthquakes in a specified space and time window with magnitude greater than or equal to M. Constant a describes the seismic productivity of the region and b or b-value describes the occurrence ratio of small to large earthquakes in the region. The b-values varies from region to region but typically it ranges from 0.6 to 1.4 with a global mean of about 1.0 (Udias, 1999). A b-value greater than 1.0 indicates areas of crustal heterogeneity and low applied stress, whereas values lower than 1.0 indicates crustal homogeneity and high differential stress (Wyss, 1973; Wiemer and Katsumata, 1999; Wiemer and Wyss, 2002; Yadav, 2009; Yadav et al., 2011).

The constants a and b for this sequence have been evaluated from ZMAP software (Wiemer, 2001). The b-value was obtained from maximum likelihood method (Utsu, 1978) since it gives most robust results than least-square method. The b-value was calculated from following formula:

$$b = \frac{1}{log_{10}[\overline{M} - (M_{min} - \Delta m/2)]} \tag{2}$$

where M_{min} is the minimum magnitude or threshold magnitude or magnitude of completeness (Mc) for the aftershock sequence, $\overline{M}$ is the mean magnitude and Δm is the magnitude resolution. The threshold magnitude (M_{min}) is one of the most important parameter

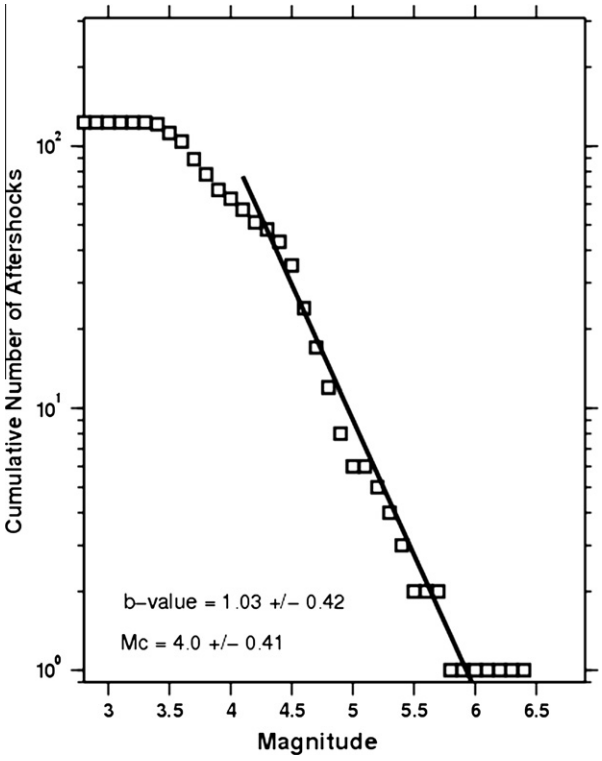

Fig. 3. Frequency–magnitude distribution of G–R relationship ($\log_{10} N = a - bM$) from which b-value (1.03 ± 0.42) is computed for 0.1 magnitude interval using maximum likelihood estimation method. Mc (4.0 ± 0.41) shows the magnitude of completeness.

calculated from frequency–magnitude distribution curve indicating the completeness of the dataset. In this study, M_{min} has been calculated from maximum curvature method (Woessner and Weimer, 2005). The errors on the parameters have been evaluated by the bootstrapping techniques of Efron and Tibshirani (1993). The threshold magnitude (M_{min}) for Baluchistan sequence was found equal to 4.0 ± 0.41 with 90% goodness of fit level (Fig. 3). The a and b-values for this sequence were found equal to 5.77 ± 0.70 and 1.03 ± 0.42, respectively. The b-value is closer to the global mean value of 1.0 which reveals the tectonic genesis of this sequence. Yadav (2009) and Yadav et al. (2010) observed low b-value of 0.66 in the Pakistan region for background seismicity. Thingbaijam et al. (2009) also reported low b-value of 0.81 in Pakistan region calculated from background seismicity.

4.2. Relationship between magnitude of main shock and its largest aftershock

The level of aftershocks is mainly related with the size of main shock in a seismic sequence (Utsu, 2002a). The stress condition and heterogeneity of rock mass affect the size difference (Δm) between magnitude of main shock (M_0) and its largest aftershock (M_1). According to Bath (1965), generally, this size difference shows a constant value ($\Delta m = 1.2$) and does not depend upon the size of main shock which implies that the stress transfer responsible for the occurrence of aftershocks is a self-similar process (Utsu, 2002a; Shcherbakov and Turcotte, 2004). A number of studies have been carried out to show the statistical variability of this law (Kisslinger and Jones, 1991; Tsapanos, 1990; Felzer et al., 2002, 2003; Console et al., 2003; Helmstetter and Sornette, 2003; Yadav et al., 2005, 2011). However, its validity remains an open question, regardless of the progress of understanding the characteristics of

Bath's law. Utsu (2002a) observed that Δm varies from 0 to 3 or more for earthquake sequences in Japan and mainly depends upon the regional characteristics of the study area.

The largest aftershock in the Baluchistan earthquake sequence occurred on December 9, 2008 of magnitude Mw 5.7 (Table 1, Fig. 2). In this sequence, the difference between magnitude of main shock and its largest aftershock (Δm) is observed as 0.7, which is much lower than the actual difference of 1.2 according to the Bath's law. This indicates that Baluchistan earthquake sequence does not follow the original Bath's law, making its seismic characteristics different than the other worldwide observed seismic sequences. Papazachos et al. (1967) observed difference of 0.67 for the earthquake sequences of magnitude 6.0 in Greece. Shcherbakov et al. (2005) also observed the difference as low as 0.8 for January 17, 1994 Northridge earthquake of magnitude Mw 6.4. The ratio of magnitude of largest aftershock (M_1) and main shock (M_0) in Baluchistan sequence is calculated as 0.89 which is rather high implying heterogeneous rock mass within the seismogenic volume (Gupta and Rastogi, 1976; Yadav et al., 2011).

Shcherbakov and Turcotte (2004) proposed a modified form of Bath's law which is based on extrapolation of G–R relationship for aftershocks. They obtained the largest aftershock magnitude M^* from G–R relationship (Eq. (1)) by setting $N(\geqslant M) = 1$ and then calculating M^* from following formula:

$$M^* = \frac{a}{b} \tag{3}$$

Then, if Bath law is applicable, the modified Bath's law can be written as:

$$\Delta m^* = M_0 - M^* \tag{4}$$

where Δm^* is apparently a constant. The G–R relationship (Eq. (1)) can be written in the following form using Eqs. (3) and (4):

$$\log_{10} N(\geqslant M) = b(M_0 - \Delta m^* - M) \tag{5}$$

The frequency–magnitude distribution can be described from above Eq. (5) with the help of parameters b, M_0 and Δm^*. Shcherbakov and Turcotte (2004) explained the general applicability of modified Bath's law and analyzed the partitioning of the released seismic energy between main shock and aftershocks and its relation to Δm^*. They observed that the ratio of total energy radiated in an aftershock sequence to the energy radiated by main shock is constant. They used the following energy relation given by Utsu (2002b):

$$\log_{10} E(M) = \frac{3}{2}M + \log_{10} E_0 \tag{6}$$

where E_0 has a constant value of 6.3×10^4 Joules (Utsu, 2002b) and M is the moment magnitude.

They obtained the following formula for the estimation of ratio between total radiated energy for aftershocks (E_{AS}) and radiated energy of main shock (E_{M0}):

$$\frac{E_{AS}}{E_{M0}} = \frac{b}{\frac{3}{2} - b} 10^{-\frac{3}{2}\Delta m^*} \tag{7}$$

Then, the fraction of total energy associated with aftershocks can be written as (Shcherbakov et al., 2005):

$$\frac{E_{AS}}{E_{M0} + E_{AS}} = \frac{\frac{b}{\frac{3}{2}-b} 10^{-\frac{3}{2}\Delta m^*}}{1 + \frac{b}{\frac{3}{2}-b} 10^{-\frac{3}{2}\Delta m^*}} \tag{8}$$

We applied Shcherbakov and Turcotte (2004) method of modified Bath's law for the Baluchistan sequence. Considering $a = 5.77$ and $b = 1.03$ from G–R relationship for this sequence, we obtained the modified magnitude of largest aftershock (M^*) as 5.6 and magnitude difference (Δm^*) as 0.8 following Eqs. (3) and (4), respectively. The values of magnitude difference obtained from modified Bath's law differs 0.1 unit from original Δm. Taking $b = 1.03$ and $\Delta m^* = 0.8$, we found that 12% of the total energy is associated with the aftershocks activity while 88% is associated with main shock. Shcherbakov and Turcotte (2004) obtained the values of $E_{AS}/(E_{M0} + E_{AS})$ of Eq. (8) for ten largest earthquake sequences in California and constructed a graph showing relationship between $E_{AS}/(E_{M0} + E_{AS})$ and Δm^* for different b-values of 0.8, 1.0 and 1.2 to see the dependence of these parameters on each other. We estimated the value of $E_{AS}/(E_{M0} + E_{AS})$ as 0.11 form Eq. (8) using $b = 1.03$ and $\Delta m^* = 0.8$ for this sequence which fits well in the graph provided by Shcherbakov and Turcotte (2004) for b-value of 1.0. This reveals that the property of radiated seismic energy for Baluchistan earthquake sequence is similar to the California earthquake sequences.

4.3. Temporal decay of aftershocks

The modified form of Omori's law (Utsu, 1961) describes the temporal decay of aftershocks (Utsu et al., 1995; Utsu, 2002a; Scholz, 2002):

$$N(t) = \frac{K}{(c+t)^p} \tag{9}$$

where $N(t)$ is the rate of occurrence of aftershocks, t is the time elapsed since main shock and K, p and c are empirical constants. This law is an expression of temporal correlations in aftershock sequences which can be viewed as a complex relaxation processes occurring after main shock. The constant K depends upon the total number of events in a sequence, i.e. aftershocks productivity and c on the rate of activity in the earliest part of the sequences (Utsu et al., 1995). The parameter c is influenced from the incomplete detection of small aftershocks in the early stage of the sequence (Kisslinger and Jones, 1991). The constant p describes the steepness of the decay of aftershocks and is represented by the slope of the double-logarithmic plot of the number of aftershocks per unit time and the time after the main shock. In original Omori's law, Omori (1894) used the value of p as 1 which is global value for any aftershock sequence. Generally, p varies in the range of 0.9–1.5 (Utsu et al., 1995) and depends upon the structural heterogeneity, stress and temperature in the crust.

The maximum-likelihood method is used to estimate the values of constant K, p and c of Eq. (9) for Baluchistan sequence and illustrated in Fig. 4. A p-value 0.89 ± 0.07 was estimated for this sequence which is rather low as compared to the global p-value of 1.0. The low p-values for Baluchistan sequence reveals slow decay of aftershocks activity. Bowman (1997) observed that the temporal decay of aftershock activity shows the stress dissipation with time in the aftershock region in Australia. Kisslinger and Jones (1991) correlated high p-values with high values of heat flow for California and suggested that higher temperature causes shortened stress relaxation times for the fault zone. The slow decay rate of aftershocks activity in Baluchistan sequence can be attributed with the low surface heat flux in the epicentral region. Low surface heat causes longer stress relaxation times in the fault zone. The above can be considered as a fiducial explanation for the low p-value estimated in the present study.

Following Ogata (1999), we used the observed data of occurrence time of aftershocks of learning period (t_L) of 20 days to fit the parameters (K, c, p) of four models of modified Omori law (Woessner et al., 2004) applying the maximum likelihood method and forecasted the aftershocks activity for next 43 days (t_F). We used the best model to forecast the aftershocks activity until the end of the forecasted period (t_F). Ogata (1999) assumed that the aftershocks sequence is distributed according to a nonstationary Poisson process. The modified Omori model (Eq. (9)) is the basic model among four models whereas other three models consist of

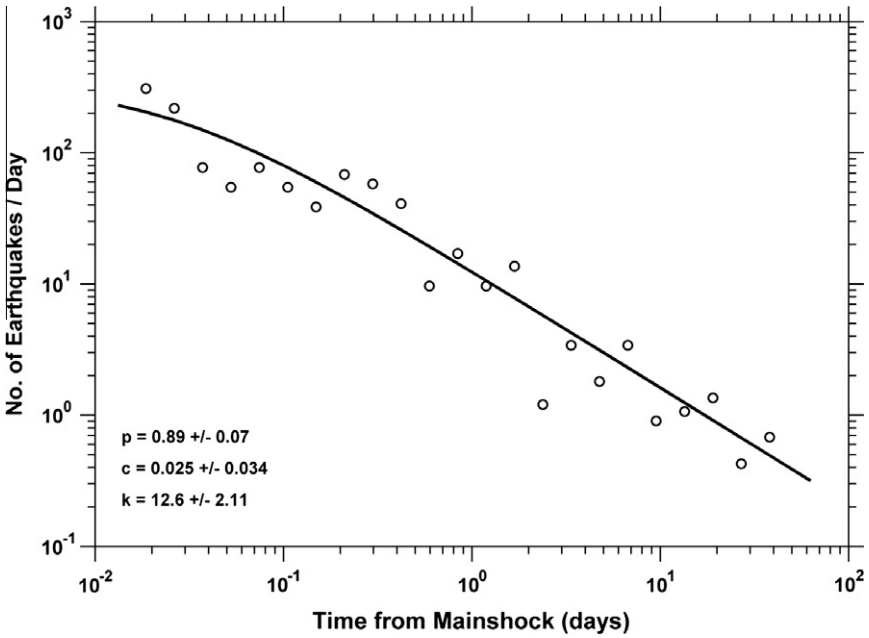

Fig. 4. Number of aftershocks ($N \geqslant Mc$) after the occurrence of main shock showing occurrence rate of aftershocks as a function of elapsed time. The fit of the K, c, and p parameters of modified Omori law was performed.

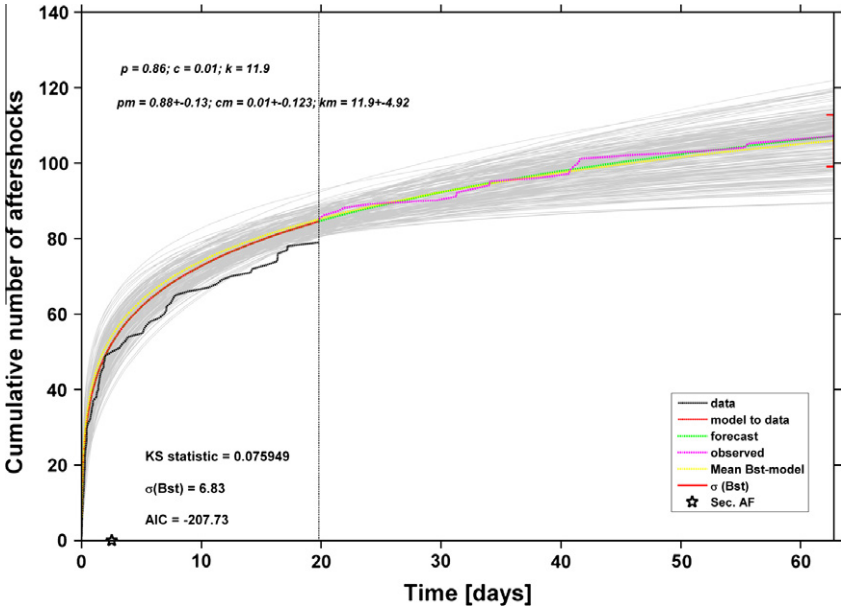

Fig. 5. Forecast model of aftershocks activity based on observed data of 20 days learning period estimated using maximum likelihood method. Figure shows modified Omori law fits with the bootstrap forecast models plotted as gray lines in the background, the green line displaying the mean forecast model and the red bar indicating the standard deviation of forecasted events at forecasted time (t_F). The vertical line indicates the end of the learning period t_L. Star at time axis shows second aftershock in learning period. (For interpretation of the references to color in this figure legend, the reader is referred to the web version of this article.)

one secondary aftershock sequence within the learning period (Woessner et al., 2004). We applied simpler modified Omori model for forecasting aftershocks following suggestions of Woessner et al. (2004). The intensity function of these Omori models is written as (Woessner et al., 2004):

$$\lambda(t) = \lambda_1(t) = K_1(t + c_1)^{-p1} \quad t < t_a$$

and

$$\lambda(t) = \lambda_2(t) = K_1(t + c_1)^{-p1} + K_2(t + c2)^{-p2} \quad t_a \geqslant t \geqslant t_L \qquad (10)$$

where t_a is the time of largest aftershock from the main shock time in learning period. The indices 1 and 2 in Eq. (10) are related with the parameters of modified Omori law in the time periods before and after the occurrence of largest aftershocks at t_a in the learning time period, respectively. We fit four models given by Woessner et al. (2004) varying as a function of free parameters (K, p, c, K_1, p_1, c_1, K_2, p_2 and c_2). We used the corrected Akaike Information Criterion AIC_c (Kenneth et al., 2002) to test the best fitting model:

$$AIC_c = -2max(lnL) + 2(p) + 2p(P + 1)/N - P - 1 \qquad (11)$$

where $ln(L)$ is likelihood function, P is the number of free parameters and N is the sample size. AIC_c is used to select the best model. Even if all the models are poor, AIC_c still selects the one estimated to be best, but even that model may be poor in an absolute sense (Kenneth et al., 2002). Thus, we estimate the goodness-of-fit for the selected AIC_c model to the observed data by applying a Kolmogorov–Smirnov-Test at a significance level of 0.05 (Conover, 1999). The uncertainty in the model forecast at time t_F is based on the bootstrap approach. The original dataset is bootstrapped for 100 times and model parameters and forecast are estimated at each bootstrap time.

The estimated model parameters and forecasting for aftershocks for Baluchistan sequence is shown in Fig. 5. The learning period t_L has been taken as 20 days from the beginning of main shock. The largest aftershock in learning period is shown with star on time axis which is used to separate learning period in two periods before and after the time of occurrence of aftershock to fit the modified Omori's model parameters. The parameters of modified Omori model were estimated as $p = 0.88 \pm 0.13$, $c = 0.01 \pm 0.123$, and $K = 11.9 \pm 4.92$ after fitting the best model showing good agreement with observed parameters. The forecast of aftershocks activity for next 43 days on the basis of modeled parameters of 20 days learning period shows good agreement with the observed aftershocks activity and forecasted curve falls within the standard deviation (σ) of forecasted events at the time of t_F (Fig. 5). This type of forecasting of aftershocks activity can take a lead role in the short-term aftershocks hazard assessment in any region of the world.

4.4. Spatial fractal dimension (D_s)

The spatial clustering of earthquakes is examined through the spatial fractal dimension (D_s). It describes the spatial distribution of earthquakes and provides strength of spatial clustering. It implies that smaller the fractal dimension, smaller is the spatial clustering and vice-versa. In this study, we used correlation integral method for fractal analysis (Grassberger and Procaccia, 1983) in order to investigate the spatial properties of aftershock sequence of Baluchistan sequence.

According to Grassberger and Procaccia (1983), the correlation integral of distribution of N earthquakes is:

$$C(R) = \frac{2N_{R<r}}{N(N-1)} \tag{12}$$

where N ($R < r$) is the number of event pairs separated by a distance R smaller than r. If the distribution is fractal, then:

$$C(r) \sim r^{D_s} \tag{13}$$

where D_s is the spatial fractal dimension. The fractal dimension of a spatial distribution of earthquakes can be estimated as the slope of the best–fitted straight line into the log–log plot of $C(r)$ versus r. The variation in fractal dimension in different zones gives a lot of information about the geological heterogeneity and stability of the region (Dimitriu et al., 1993; DeRubeis et al., 1993). The fractal dimension of spatial distribution of hypocenters is related with the heterogeneity of the fractured material. It characterizes the degree to which the fractals fill up the surrounding space. A D_s-value close to zero may be interpreted as all events clustered into one point, close to 1 indicates the dominance of line sources, close to 2 indicates the planar fractured surface being filled up and a value close to 3 indicates that earthquake fractures are filling up a crustal volume (Khattri, 1995; Yadav et al., 2011).

We estimated spatial fractal dimension for Baluchistan sequence from the double–logarithmic plot of the correlation integral and distance between hypocenters (Fig. 6), and found it equal to 2.08 ± 0.02. The D_s-value of 2 indicates that the events are randomly distributed into the two-dimensional fault plane that is being filled up by fractures. This value can be adjudged as indicative for approaching a two-dimensional region. The relation between the fractal dimension, D_s and b-value is widely discussed by various researchers (Aki, 1981; Khattri, 1995; Wyss et al., 2004; Yadav et al., 2011). Aki (1981) first showed that these two parameters are related as $D = 3b/c$, where $c \approx 1.5$ is the scaling constant between the logarithm of the moment and magnitude of an earthquake (Kanamori and Anderson, 1975). In this study, with $D_s = 2.08$ and $b = 1.03$, we found that $c = 1.49$, which is in good agreement with the aforementioned statements.

5. Coseismic Coulomb stress changes and triggering of seismic activity

Earthquakes occur when the stress exceeds the strength of the rocks of the fault (Scholz, 2002). The closeness to failure of a fault is computed using the changes in the Coulomb stress, sometime referred as a function known as Coulomb Failure Function (ΔCFF). It depends on the changes in both shear stress and normal stress,

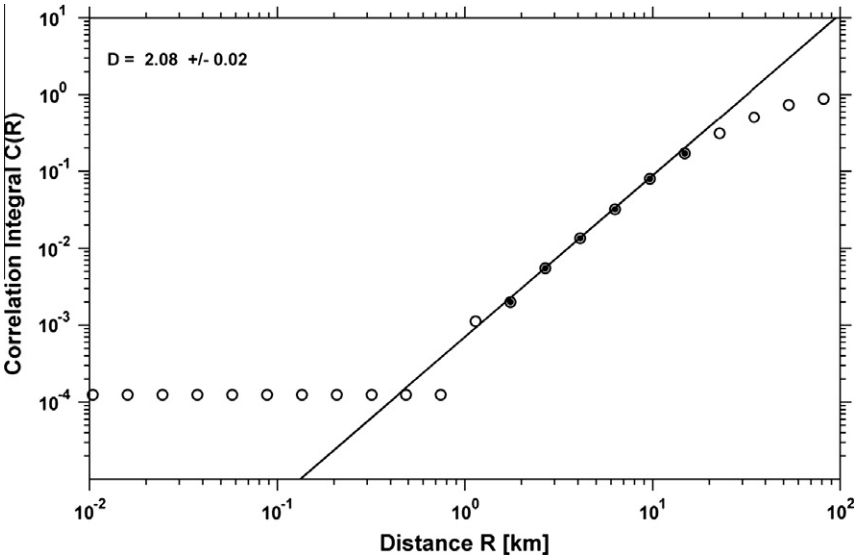

Fig. 6. Graph shows the fractal dimension (*Ds*) of the aftershocks distribution. Solid circles show the data for which best fit is performed for the computation of *D*-value.

and in the presence of pore pressure it can be expressed as (King et al., 1994; Stein et al., 1994; Harris, 1998; Toda et al., 1998; King and Cocco, 2000; Freed, 2005; Rajput et al., 2005; Raju et al., 2008):

$$\Delta CFF = \Delta\tau + \mu(\Delta\sigma_n + \Delta P) \quad (14)$$

where $\Delta\tau$ is the shear stress changes resolved on a given failure plane (positive in the direction of fault slip), $\Delta\sigma_n$ is the normal stress changes (positive if compressive), ΔP is the pore pressure changes in the fault and μ is the coefficient of friction that ranges from 0.6 to 0.8 for most rocks (Harris, 1998 and references therein). In this study, we ignore the time dependent changes in pore fluid pressure and considered only undrained case. According to Rice and Cleary (1976), the changes in pore pressure (ΔP) under undrained condition can be written as:

$$\Delta p = -B\frac{\Delta\sigma_{kk}}{3} \quad (15)$$

where B is the Skempton's coefficient, $(0 \leqslant B < 1)$, and $\Delta\sigma_{kk}$ indicates summation over the diagonal elements of the stress tensor. If the air fills the pores then B is nearly zero, whereas if water fills the pores, it is typically between 0.5 and 1.0 for fluid–saturated rock and close to 1.0 for fluid-saturated soil. We assume a $B = 0.5$ and $\mu = 0.75$ (as in Robinson and McGinty, 2000; among others). The apparent coefficient of friction is defined as $\mu' = \mu(1 - B)$, if in the fault zone, $\Delta\sigma_{11} = \Delta\sigma_{22} = \Delta\sigma_{33}$, so that $\Delta\sigma_{kk}/3 = \Delta\sigma$. The above selected values for B and μ result to a value of apparent coefficient of friction close to 0.4, which is widely used in studies of Coulomb stress modeling.

A positive value of ΔCFF for a particular fault denotes movement of that fault towards failure, i.e. the likelihood that it will rupture in an earthquake is increased. The Coulomb stress changes depend upon the geometry and slip of the earthquake, the geometry and sense of slip of the fault or of surface of interest (optimally-oriented plane), regional stress and apparent coefficient of friction. Generally the changes in Coulomb stress range between 0.1 and 1 bar, which are considered enough to trigger the future earthquakes. Stein (2004) found that tidal stress change is of the order of 0.01 bar and is capable of earthquake triggering. Similarly Ziv and Rubin (2000) found no lower threshold for stress triggering. It is only the delay in triggering which depends upon the amount of stress change.

5.1. Triggering of Baluchistan main shock and its doublet

We investigated the coseismic Coulomb stress changes due to the foreshock of magnitude Mw 5.3 occurred about 20 km SE of the main shock epicenter. The coseismic Coulomb stress changes due to foreshock have been modeled in an elastic half-space assuming a uniform slip distribution on the rupture plane (Figs. 2 and 7). The NW–SE trending plane is considered as the fault plane of foreshock, considering the similar strike of the mapped Urghargai Fault and aftershocks activity. The well-known empirical relationships developed by Wells and Coppersmith (1994) have been used to calculate the subsurface rupture length (=4.48 km) and subsurface rupture width (=3.79 km). The right-lateral strike-slip component and reverse slip component was computed as 18 cm and 7.3 cm, respectively using the relation $M_0 = \mu AD$, assuming a shear modulus (μ) of 3.2×10^5 bars (Stein et al., 1994). For all the calculations, we used the Poisson ratio (v) 0.25 and effective coefficient of friction (μ') 0.40 (Harris, 1998; Papadimitriou and Sykes, 2001; Papadimitriou, 2002). We calculated Coulomb stress changes at the centroid depth of foreshock (16.6 km) for a NW–SE oriented right-lateral strike-slip fault (Fig. 7). The Coulomb stress changes due to foreshock are calculated on the right-lateral strike slip receiver fault of the main shock (strike = 304°, dip = 73° and rake = 171°). Fig. 7 shows the evolution of Coulomb stress field in the epicentral region of foreshock. The stress-increased or bright zone can accelerate the seismicity while the stress-shadow zone can decelerate. It is observed that the Baluchistan main shock of

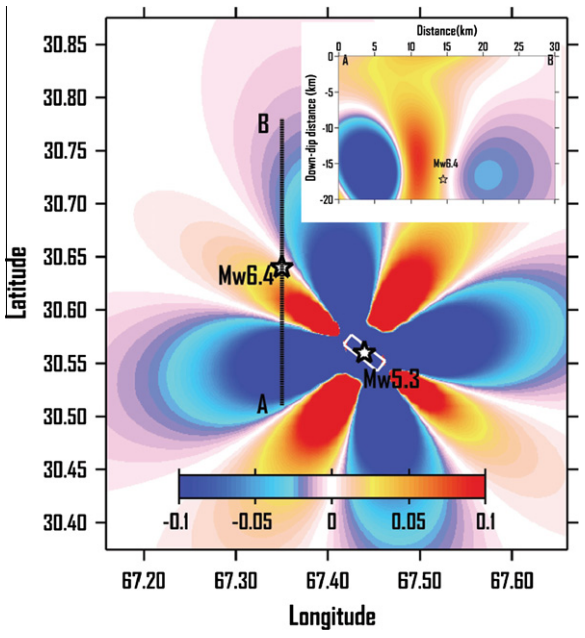

Fig. 7. Coseismic Coulomb stress changes (in bars) due to foreshock (Mw 5.3), occurred about 40 min before the main shock (Mw 6.4), resolved at depth 17.2 km (depth of mainshock) for specific fault plane of receiver fault of main shock (strike = 304° dip = 73°, slip = 171°) considering coefficient of friction 0.75 and Skempton's coefficient 0.5. Figure in inset shows the cross-sectional view of Coulomb stress due to foreshock along line AB. The occurrence of mainshock (Mw 6.4) in positive Coulomb stress region shows that it was triggered due to foreshock.

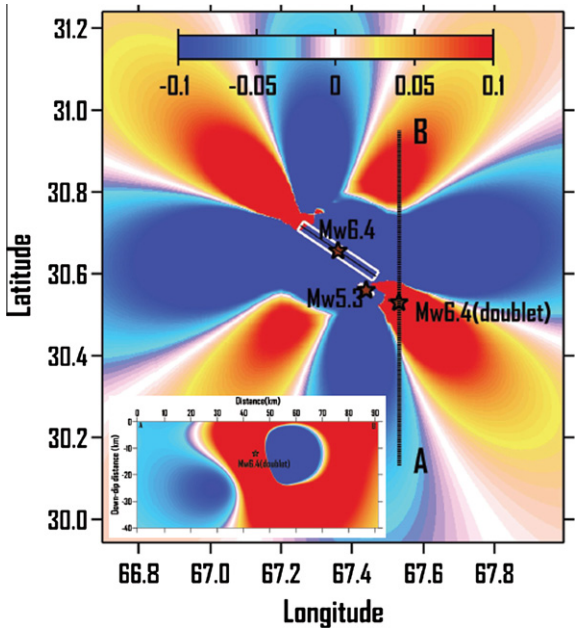

Fig. 8. Coseismic Coulomb stress changes (in bars) due to foreshock (Mw 5.3) and main shock (Mw 6.4) resolved on specific fault plane of receiver fault of main shock doublet Mw 6.4 (strike = 324° dip = 68°, slip = −178°) considering coefficient of friction 0.75 and Skempton's coefficient 0.5. Figure in inset shows the cross-sectional view of Coulomb stress due to foreshock and mainshock along line AB. The occurrence of mainshock doublet (Mw 6.4) in positive Coulomb stress shows that it was triggered due to transfer of positive Coulomb stress from coseismic slip of foreshock and mainshock.

magnitude Mw 6.4 occurred in the lobe of increased Coulomb stress which shows that main shock was promoted to failure due the transfer of positive Coulomb stress by coseismic slip of foreshock and thus triggered by foreshock. The calculated Coulomb stress changes due to foreshock, in a cross-section along line AB passing through epicenter of main shock, show that the main shock hypocenter is located in positive stress region sandwiched between low stress regions, evidencing the triggering of main shock due to foreshock. The above results do not affect significantly due to variation in ±0.2 units in the coefficient of friction (μ) and Skempton's coefficient (B) from $\mu = 0.75$ and $B = 0.5$ suggesting that our results are robust.

We also investigated the Coulomb stress changes due to combined coseismic rupture of foreshock and mainshock (Fig. 8). The NW–SE oriented plane was selected as the likely failure plane of mainshock. However, McCloskey and Nalbant (2009) selected failure plane oriented in the NE–SW direction which was assumed on the basis of the regional structure visualized in the topography of the source region. The centroid depth of mainshock was considered as 17.2 km. The calculation was performed considering the subsurface length and width of the mainshock fault rupture as 24.51 km and 10 km respectively, the right-lateral slip component as 58.9 cm and reverse slip component of 9.3 cm estimated using empirical relationships of Wells and Coppersmith (1994). GPS measurement in the epicentral region (Khan et al., 2008) are consistent with 62 cm and 60 cm coseismic right-lateral strike slip associated with the mainshock and its doublet respectively, which are also consistent with our modeled values of coseismic slip. The Coulomb stress changes due to foreshock and mainshock was calculated on the right-lateral strike-slip receiver fault of the main shock doublet (strike = 324°, dip = 68° and rake = −178°). Fig. 8 shows the evolution of Coulomb stress due to coseismic slip of foreshock and mainshock. It is observed that hypocenter of the mainshock doublet (Mw 6.4) lies within the increased Coulomb stress region towards SE of mainshock rupture, suggesting that the failure of mainshock doublet fault was promoted by transfer of positive Coulomb stress due to coseismic slip of foreshock and mainshock fault rupture. It implies that the mainshock doublet was triggered by the foreshock and the mainshock rupture, as also opined by McCloskey and Nalbant (2009).

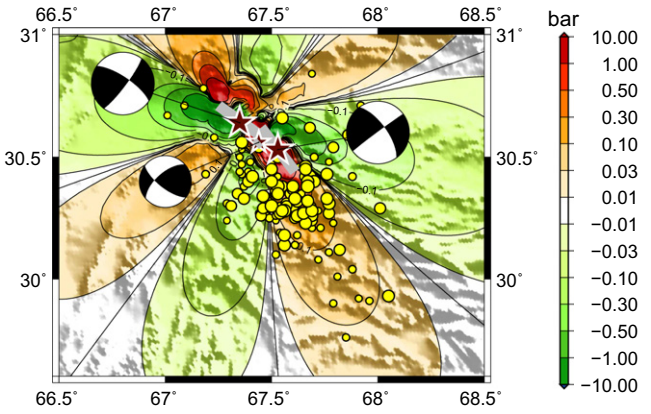

Fig. 9. Combined coseismic Coulomb stress changes (in bars) due to the foreshock (Mw 5.3), mainshock (Mw 6.4) and mainshock doublet (Mw 6.4) within depth range of 0–20 km for effective coefficient of friction 0.4 and it is resolved on optimally-oriented fault plane for strike-slip whose principal axis oriented towards NNE direction, i.e. the direction of Indian plate movement. The locations of aftershocks occurred during the period October 28–December 31, 2008 are shown with solid circles. Focal mechanism solutions for foreshock and mainshocks doublet are also shown by beach ball. It is observed that maximum number of aftershocks fall in the region of positive Coulomb stress towards SE of main shock rupture evidencing possible triggering of these aftershocks due to transfer of positive Coulomb stress.

5.2. Triggering of aftershocks activity

The Baluchistan mainshocks (Mw 6.4) was followed by a number of aftershocks during the period October 28, 2008–December 31, 2008. The epicentral distribution of the aftershocks suggests that the causative faults of the main shock and its doublet are aligned in the NW–SE directions which were activated during the seismic excitation. We calculated coseismic Coulomb stress changes due to the foreshock, main shock and its doublet to analyse the correlation between increased Coulomb stress regions and locations of aftershocks activity (Fig. 9). The coseismic Coulomb stress changes were resolved on optimally-oriented plane of strike-slip faults whose principal axis oriented towards NNE direction. The fault plane solutions of earthquakes in this region (Verma et al., 1980) and fault motion inferred from tectonic setting (Bernard et al., 2000) confirm the selection of this failure plane. The resultant Coulomb stress modeling for the foreshock, main shock and its doublet for depth range 0–20 km is shown in Fig. 9 with aftershock activity of magnitude $m_b \geqslant 3.0$ occurred during the period October 28–December 31, 2008. It appears that the aftershock locations are moderately correlated with the area of increased Coulomb stress towards SE of the Baluchistan mainshocks rupture. It is observed that Coulomb stress increase do not just occur at the fault-ends but also in off-fault regions. Most of the aftershock activity is related with southeastern lobe of increased Coulomb stress due to the concentration of slip at fault-ends where rupture terminates. The stress pattern is controlled by both initiation and termination ends of the main fault rupture. The off-fault aftershock triggering is observed in the lobe near the fault termination (Fig. 9), which is most likely caused by shear stress increase observed by several researchers (Das and Scholz, 1981; Stein et al., 1994; Harris, 1998; Stein, 1999; Karakostas et al., 2003, 2004). The occurrence of majority of aftershock activity in the southeastern part of rupture suggests that the slip was propagated towards SE of the main shock rupture and concentrated at the end of fault-rupture.

For the aftershocks study, the correlation between increased Coulomb stress region and locations of observed aftershocks is not so perfect and about 75% of the total aftershocks occurred in the increased zone. Some aftershocks occurred in the region of decreased Coulomb stress (stress shadow region). However, we accept that there could be an error of about 10 km in the hypocentral locations of these aftershocks. Ideally a few aftershocks or triggered earthquakes should occur in such regions if the Coulomb hypothesis is valid (Harris and Simpson, 1996). The occurrence of aftershocks activity in stress shadow regions is generally due to oversimplifications of modeled fault-slip, unaccounted of heterogeneity of crust and existence of small faults with different azimuthal orientations. Generally, the best correlation between increased Coulomb stress and locations of aftershocks is observed at distances greater than a few kilometers from the fault rupture (Freed, 2005). The slip distribution and rupture geometry influence the near-fault stress changes. Further, we have assumed that all the aftershocks occurred due to static stress change caused by the earthquake sequence. The relaxation of stresses, mostly due to poroelastic effects as the short time duration is considered, may also modify the stress state.

6. Discussion and conclusions

The seismotectonic properties and sequential seismicity triggering due to the Coulomb stress transfer for Baluchistan earthquake sequence have been studied in order to examine the seismic characteristics of the region. For this purpose, statistical properties such as seismic b-value of G–R relationship, relationship

between magnitude of main shock and largest aftershock (modified Bath's law), partitioning of radiated seismic energy due to aftershocks activity, *p*-value, forecasting of aftershocks activity, *D*-value and Coulomb stress transfer have been calculated and analyzed using aftershocks data from NEIC catalog during the period October 28–December 31, 2008. The Baluchistan sequence exhibited the complexity of present day tectonics in Pakistan, mostly thrust/fold belt along with some strike-slip faults in NNW to NW direction identified by Kazmi (1979) from field studies and satellite images. The causative fault associated with the Baluchistan earthquake sequence in NNW–SSE to NW–SE direction is in agreement with the strike of right-lateral strike slip Urghargai fault (Kazmi, 1979). The spatial distribution of aftershocks correlated with the fault plane solutions of foreshock, main shock and its doublet show that the aftershocks occurred on a steeply-dipping right-lateral strike slip fault plane oriented in NW–SE direction. The occurrence of aftershocks activity towards SE of mainshocks rupture shows that the slip propagated from NW to SE and triggered most of the aftershocks activity in this region.

The statistical properties of Baluchistan earthquake sequence have been analyzed and correlated with present tectonics and rheology of the region. The seismic *b*-value of G–R relationship for this sequence has been estimated as 1.03 ± 0.42 with magnitude of completeness 4.0 ± 0.41. The *b*-value close to global mean value of 1.0 indicates the tectonic genesis of the sequence. The normal *b*-value for Baluchistan sequence as compared to high *b*-values for worldwide aftershock sequences is due to the occurrence of larger magnitude aftershocks and paucity of smaller size aftershocks ($M \leqslant 3.0$). Thingbaijam et al. (2009) and Yadav et al. (2010) also observed low *b*-value for Pakistan region from background seismicity. The relationship between magnitude of the main shock and its largest aftershock for this sequence has been studied on the basis of modified Bath's law. It is observed that the magnitude difference is as low as 0.7, suggesting that sequence does not follow the Bath's law. Similar characteristics are also observed by Papazachos et al. (1967) for the earthquake sequences in Greece and Shcherbakov et al. (2005) for January 17, 1994 Northridge earthquake. The ratio of magnitude of largest aftershock and main shock is calculated as 0.89 which is rather high implying heterogeneous rock mass within the seismogenic volume. The partitioning of radiated seismic energy for aftershocks activity in Baluchistan sequence has been calculated using the method of Shcherbakov and Turcotte (2004) and observed that 12% of the total energy is associated with the aftershock sequence while 88% is associated with the main shock. The fraction of total energy associated with aftershocks falls at the appropriate place in the graph for earthquake sequences in California region provided by Shcherbakov and Turcotte (2004) suggesting that the aftershocks characteristics of this sequence are correlated with the California earthquake sequences.

The decay properties of Baluchistan aftershock sequence is studied in terms of *p*-value of modified Omori law. The *p*-value is observed as low as 0.89 ± 0.07 which reveals the slow decay of aftershocks activity indicating low surface heat flux in the considered region. This is due to the fact that low surface heat causes longer stress relaxation times in the fault zone (Kisslinger and Jones, 1991). The forecasting of aftershocks activity for next 43 days has been performed following Ogata (1999) and Woessner et al. (2004) method using 20 days of learning period from occurrence of main shock. The modeled forecasting and observed aftershocks activity show good agreement in the considerable standard deviation of forecasted aftershocks. This type of short-term aftershocks forecasting can be useful in mitigating the aftershocks hazard in the region for next earthquake sequences. The spatial distribution of aftershocks activity has been studied in terms of fractal dimension (D_s). The fractal dimension (D_s) equal to 2.08 ± 0.02 suggests that events are randomly distributed into a two-dimensional fault plane that is being filled up by fractures. This value can be adjudged as indicative for approaching a two-dimensional region. A positive correlation between fractal dimension (D_s) and *b*-value ($D_s = 3b/1.5$) is observed for this sequence.

The static Coulomb stress modeling has been performed to explain the sequential seismicity triggering of mainshock due to foreshock, mainshock doublet due to foreshock and mainshock, and aftershocks due to foreshock, mainshock and its doublet. Triggering does not mean that the coseismic stress changes associated with one earthquake is enough to generate another earthquake at an originally stress-free location. It means that stress at the location of the second earthquake already is close enough to failure so that the first earthquake can 'trigger' the second one or move the fault into the failure regime by introducing a small positive increase in Coulomb stress (Papadimitriou and Sykes, 2001; Papadimitriou, 2002; Rajput et al., 2005). Coulomb stress analysis for foreshock on a NW–SE oriented right-lateral strike-slip fault indicates that foreshock caused an increase in Coulomb failure stress at the main shock hypocentral area, hence promoting failure on the main shock fault. This reveals that the main shock was triggered by the transfer of positive Coulomb stress due to a foreshock. The combined Coulomb stress changes due to coseismic rupture of foreshock and mainshock suggest that mainshock doublet (Mw 6.4) was also triggered by the transfer of positive stress at the hypocenter of mainshock doublet. This is consistent with the view of Marsan and Legline (2008) who suggested that earthquake of any size can trigger earthquakes/aftershocks and may result in cascade triggering. It may be also concluded that the faults in Baluchistan region are critically stressed and even a small increase in stress (0.01–0.05 bar, as in this case) can trigger earthquakes on the faults. This is consistent with the view that there may not exist a lower threshold for earthquake triggering (Ziv and Rubin, 2000). Positive Coulomb stress changes at the hypocenter of the main shock and its doublet are also observed for different values of coefficient of friction (μ) and Skempton's coefficient (B), evidencing that our final results are not affected by these variations and appears to be robust. The correspondence between aftershocks activity and the positive Coulomb failure stress regions produced by the foreshock, main shock and its doublet are in good agreement with the previous studies that provides the potential explanation of aftershock triggering (King et al., 1994; Stein et al., 1994; Harris, 1998; Toda et al., 1998; Karakostas et al., 2003, 2004; Rajput et al., 2005; Gahalaut, 2008; Yadav et al., 2011). It is observed that the cumulative static stress changes from foreshock, main shock and its doublet and background loading rate triggered a population of secondary faults and subsequent aftershocks activity. The occurrence of mainshock doublet and aftershock activity at the southeastern end of the main shocks rupture could be interpreted as a result of end effects of slip propagation or as the site of additional fault slip. This validates the postulation of earthquake triggering in this sequence. Instead of one major rupture, two segments due to mainshocks have been failed separately due to most probably reason of fault segmentation and weak slip in foreshock.

Acknowledgements

The first author is thankful to Prof. E.E. Papadimitriou and Prof. V.G. Karakostas of Aristotle University of Thessaloniki, Greece for discussion and suggestions on the early results of this paper. Some figures were prepared using the public domain GMT software (Wessel and Smith, 1998). First author is thankful to the Director, INCOIS and HoD, ASG, INCOIS for providing infrastructure facilities. Authors are thankful to two anonymous reviewers for constructive comments and suggestions which enhanced quality of the manuscript. Indian National centre for Ocean Information Services (INCOIS) contribution no. 87.

References

Aki, K., 1981. A probabilistic synthesis of precursory phenomena. In: Symposium, D.W., Richards, P.G. (Eds.), Earthquake Prediction: An International Review. AGU, Washington, DC, pp. 566–574.

Ambraseys, N., Bilham, R., 2003. Earthquakes and associated deformation in Northern Baluchistan 1892–2001. Bulletin of the Seismological Society of America 93 (4), 1573–1605.

Bath, M., 1965. Lateral inhomogeneities in the upper mantle. Tectonophysics 2, 483–514.

BCP, 2007. Building Code of Pakistan (Seismic Provisions 2007). Ministry of Housing and Works, Government of Pakistan, Islamabad.

Bernard, M., Shen-Tu, B., Holt, W.E., Davis, D.M., 2000. Kinematics of active deformation in the Sulaiman Lobe and Range, Pakistan. Journal of Geophysical Research 105, 13253–13297.

Bordet, P., 1978. The western border of the Indian plate: implications for Himalayan geology. Tectonophysics 51, T71–T76.

Boulin, J., 1981. Afghanistan structure, greater India concept and eastern Tethys evolution. Tectonophysics 72, 261–287.

Bowman, J.R., 1997. A seismicity precursor to a sequence of Ms 6. 3-6.7 Midplate earthquakes in Australia. Pure Applied Geophysics 149, 61–78.

Conover, W.J., 1999. Practical Nonparametric Statistics. John Wiley, New York.

Console, R., Lombardi, A.M., Murru, M., Rhoades, D. (2003), Bath's Law and the Self-similarity of Earthquakes, Journal of Geophysical Research 108(B2), 2128.

Das, S., Scholz, C.H., 1981. Off-fault aftershock clusters caused by shear stress increase? Bulletin of the Seismological Society of America 71, 1669–1675.

DeRubeis, V., Dimitriu, P., Papadimitriou, E., Tosi, P., 1993. Recurrent patterns in the spatial behavior of Italian seismicity revealed by the fractal approach. Geophysical Research Letters (20/18), 1911–1914.

Dimitriu, P.P., Papadimitriou, E.E., Papazachos, B.C., Tsapanos, T.M., 1993. Global study of the distribution of earthquakes in space and in time by the fractal method. In: Proceedings of the 2nd Congress Hellenic Geophysics Union, vol. 1. May 5–8, Florina, pp. 164–174.

Efron, B., Tibshirani, R., 1993. An Introduction to the Bootstrap. Monographs on Statistics and Applied Probability, vol. 57. Chapman and Hall/CRC, New York.

Farah, A., Lawrence, R.D., DeJong, K.A., 1984. An overview of the tectonics of Pakistan. In: Haq, B.U., Milliman, J.D. (Eds.), Marine Geology and Oceanography of Arabian Sea and Coastal Pakistan. Van Nostrand Reinhold, New York, NY, pp. 162–176.

Felzer, K.R., Becker, T.W., Abercrombie, R.E., Ekstro, M.G., Rice, J.R., 2002. Triggering of the 1999 MW 7.1 hector mine earthquake by aftershocks of the 1992 Mw 7.3 landers earthquake. Journal of Geophysical Research 107(B9), 2190.

Felzer, K.R., Abercrombie, R.E., Ekstro, M.G., 2003. Secondary aftershocks and their importance for aftershock forecasting. Bulletin of the Seismological Society of America 93 (4), 1433–1448.

Freed, A.M., 2005. Earthquake triggering by static, dynamic, and postseismic stress transfer. Annual Review of Earth and Planetary Sciences 33, 335–367.

Gahalaut, V.K., 2008. Coulomb stress change due to 2005 Kashmir earthquake and implications for future seismic hazards. Journal of Seismology 12, 387–394.

Grassberger, P., Procaccia, I., 1983. Characterization of strange attractors. Physical Review Letters 50, 346–349.

Gupta, H.K., Rastogi, B.K., 1976. Dams and Earthquakes. Elsevier, Amsterdam. p. 229.

Gutenberg, B., Richter, C.F., 1944. Frequency of earthquakes in California. Bulletin of the Seismological Society of America 34, 185–188.

Harris, R.A., 1998. Introduction to special section: stress triggers, stress shadows and implications for seismic hazard. Journal of Geophysical Research 103 (10), 24347–24358.

Harris, R.A., Simpson, R.W., 1996. In the shadow of 1857-effect of the great Ft. Tejon earthquake on subsequent earthquakes in southern California. Geophysical Research Letters 23, 229–232.

Helmstetter, A., Sornette, D., 2003. Bath's law derived from the Gutenberg–Richter law and from aftershock properties. Geophysical Research Letters 30(20), 2069.

Ishimoto, M., Iida, K., 1939. Observations of earthquakes registered with the microseismograph constructed recently. Bulletin of the Earthquake Research Institute, University of Tokyo 17, 443–478.

Kanamori, H., Anderson, D.L., 1975. Theoretical basis of some empirical relations in seismology. Bulletin of the Seismological Society of America 65, 1073–1095.

Karakostas, V.G., Papadimitriou, E.E., Karakaisis, G.F., Papazachos, C.B., Scordilis, E.M., Vargemezis, G., Aidona, E., 2003. The 2001 Skyros, Northern Aegean, Greece, earthquake sequence: off-fault aftershocks, tectonic implications and seismicity triggering. Geophysical Research Letters 30 (1). doi:10.1029/2002GL015814.

Karakostas, V.G., Papadimitriou, E.E., Papazachos, C.B., 2004. Properties of the 2003 Lefkada Ionian Islands, Greece, earthquake seismic sequence and seismicity triggering. Bulletin of the Seismological Society of America 94, 1976–1981.

Kazmi, A.H., 1979. Active fault systems in Pakistan. In: Farah, A., DeJong, K.A. (Eds.), Geodynamics of Pakistan. Geol. Surv. Pak., Quetta, pp. 285–294.

Kenneth, P., Burnham, K.P., Anderson, D.R., 2002. Model Selection and Multimodel Inference: A Practical Information – Theoretic Approach. Springer, New York.

Khan, M.A., Bendick, R., Bhat, M.I., Bilham, R., Kakar, D.M., Khan, S.F., Lodi, S.H., Qazi, M.S., Singh, B., Szeliga, W., Wahab, A., 2008. Preliminary geodetic constraints on plate boundary deformation on the western edge of the Indian plate from TriGGnet (Tri-University GPS Geodesy Network). Journal of Himalayan Geosciences 41, 71–87.

Khattri, K.N., 1995. Fractal description of seismicity of India and inferences regarding earthquake hazard. Current Science 69, 361–366.

King, G.C.P., Cocco, M., 2000. Fault interactions by elastic stress changes: new clues from earthquake sequences. Advances in Geophysics 44, 1–38.

King, G.C.P., Stein, R.S., Lin, J., 1994. Static stress changes and the triggering of earthquakes. Bulletin of the Seismological Society of America 84, 935–993.

Kisslinger, C., Jones, L.M., 1991. Properties of aftershocks in southern California. Journal of Geophysical Research 96, 11947–11958.

Lawrence, R.D., Khan, S.H., De Jong, K.A., Farah, A., Yeats, R.S., 1981. Thrust and strike-slip fault interaction along the Chaman transform zone, Pakistan. In: Thrust and Nappe Tectonics. Spec. Publ. Geol. Soc., London, pp. 363–370.

Lisa, M., Jan, M.Q., 2010. Geoseismological study of the Ziarat (Balochistan) earthquake (doublet?) of 28 October 2008. Current Science 98 (1), 50–57.

Maqsood, S.T., Schwarz, J., 2010. Building vulnerability and damage during the 2008 Baluchistan earthquake in Pakistan and past experiences. Seismological Research Letters 81 (3), 514–525.

Marsan, D., Legline, O., 2008. Extending earthquakes' reach through cascading. Science 319, 1076–1079.

McCloskey, J., Nalbant, S.S., 2009. Near-real-time aftershock hazard maps. Nature Geoscience 2, 154–155.

Ogata, Y., 1999. Seismicity analysis through point-process modeling: a review. Pure and Applied Geophysics 155 (2–4), 471–507.

Omori, F., 1894. On after-shocks of earthquakes. J. Coll. Sci. Imp. Univ. Tokyo 7, 113–200.

Papadimitriou, E.E., 2002. Mode of strong earthquake recurrence in the central Ionian Islands (Greece): possible triggering due to Coulomb stress changes generated by the occurrence of previous strong shocks. Bulletin of the Seismological Society of America 92, 3293–3308.

Papadimitriou, E.E., Sykes, L.R., 2001. Evolution of stress field in the Northern Aegean Sea (Greece). Geophysical Journal International 146, 747–759.

Papazachos, B.C., 1971. Aftershock activity and aftershock risk in the area of Greece. Annali di Geofisica 24, 439–456.

Papazachos, B.C., Delibasis, N., Liapis, N., Moumoulidis, G., Purcaru, G., 1967. Aftershock sequences of some large earthquakes in the region of Greece. Ann. Geofis. 20, 1–93.

PMD report, 2009. Seismotectonic analysis of Ziarat, Balochistan earthquake of 29th October, 2008 by Zahid Rafi, Najeeb Ahmed & Shafiq-Ur-Rehman, Technical report no. PMD-32/2009.

Rajput, S., Gahalaut, V.K., Sahu, V.K., 2005. Coulomb stress changes and aftershocks of recent Indian earthquakes. Current Science 88 (6), 576–588.

Raju, P.S., Gahalaut, V.K., Kumar, M.R., 2008. Phodong (Sikkim) earthquake of 14 February 2006 and its aftershocks – Coulomb stress analysis. Journal of Geodynamics 46, 63–67.

Ranalli, G., 1969. A statistical study of aftershock sequences. Annali di Geofisica 22, 359–397.

Rice, J.R., Cleary, M.P., 1976. Some basic stress diffusion solutions for fluid saturated elastic porous media with compressible constituents. Reviews of Geophysics 14, 227–241.

Robinson, R., McGinty, P., 2000. The enigma of the Arthur's Pass, New Zealand, earthquake –2. The aftershock distribution and its relation to regional and induced stress fields. Journal of Geophysical Research 105 (B7), 16139–16150.

Rowlands, D., 1978. The structure and seismicity of a portion of the southern Sulaiman Range, Pakistan. Tectonophysics 51, 41–56.

Scholz, C.H., 2002. The Mechanics of Earthquakes and Faulting, second ed. Cambridge University Press, Cambridge.

Shcherbakov, R., Turcotte, D.L., 2004. A modified form of Bath's law. Bulletin of the Seismological Society of America 94 (5), 1968–1975.

Shcherbakov, R., Turcotte, D.L., Rundle, J.B., 2005. Aftershocks statistics. Pure and Applied Geophysics 162, 1051–1076.

Stein, R.S., 1999. The role of stress transfer in earthquake occurrence. Nature 402, 605–609.

Stein, R.S., 2004. Tidal triggering caught in the act. Science 305, 1248–1249.

Stein, R.S., King, G.C.P., Lin, J., 1994. Stress triggering of the 1994 M = 6. 7 Northridge, California earthquake by its predecessors. Science 265, 1432–1435.

Tapponnier, P., Mattauer, M., Proust, F., Cassaigneau, C., 1981. Mesozoic ophiolites, sutures, and large-scale movements in Afghanistan. Earth Planetary Science Letters 52, 355–371.

Thingbaijam, K.K.S., Chingtham, P., Nath, S.K., 2009. Seismicity in the north-west frontier province at the Indian–Eurasian plate convergence. Seismological Research Letters 80 (4), 599–608.

Toda, S., Stein, R.S., Reasenberg, P.A., Dieterich, J.H., 1998. Stress transferred by the Mw = 6. 5 Kobe, Japan, shock: effect on aftershocks and future earthquake probabilities. Journal of Geophysical Research 103, 24543–24565.

Tsapanos, T.M., 1990. Spatial-distribution of the difference between the magnitudes of the main shock and the largest aftershock in the circum-pacific belt. Bulletin of the Seismological Society of America 80 (5), 1180–1189.

Udias, A., 1999. Principles of Seismology. Cambridge University Press, New York.

Utsu, T., 1961. Aftershocks and earthquake statistics. Journal of the Faculty of Science, Hokkaido University, Japan 7, 130–195.

Utsu, T., 1978. Estimation of parameter values in the formula for the magnitude–frequency relation of earthquake occurrence. Zisin (J Seism Soc Japan) 31, 367–382.

Utsu, T., 2002a. Statistical features of seismicity. In: Lee, W.H.K., et al. (Eds.), International Handbook of Earthquake and Engineering Seismology Part A. Academic Press, pp. 719–732.

Utsu, T., 2002b. Relationship between magnitude scales. In: Lee, W.H.K., Kanamori, H., Jennings, P.C., Kisslinger, C. (Eds.), International Handbook of Earthquake and Engineering Seismology, vol. Part A. Academic Press, Amsterdam, pp. 733–746.

Utsu, T., Ogata, Y., Matsuura, R.S., 1995. The centenary of the Omori formula for a decay law of aftershock activity. Journal of Physics of the Earth 43, 1–33.

Verma, R.K., Mukhopadhyay, M., Bhanja, A.K., 1980. Seismotectonics of the Hindukush and Baluchistan Arc. Tectonophysics 66, 301–322.

Wells, C., Coppersmith, K., 1994. New empirical relationships among magnitude, rupture length, rupture width, rupture area and surface displacement. Bulletin of the Seismological Society of America, 84: 974–1002.

Wessel, P., Smith, W.H.F., 1998. New, improved version of the generic mapping tools released. EOS Transactions of American Geophysical Union 79, 579.

Wiemer, S., 2001. A software package to analyze seismicity: ZMAP. Seismological Research Letters, 373–382.

Wiemer, S., Katsumata, K., 1999. Spatial variability of seismicity parameters in aftershock zones. Journal of Geophysical Research 104, 13135–13151.

Wiemer, S., Wyss, M., 2002. Spatial and temporal variability of the b-value in seismogenic volumes: an overview. Advances in Geophysics 45, 259–302.

Woessner, J., Wiemer, S., 2005. Assessing the quality of earthquake catalogues: estimating the magnitude of completeness and its uncertainty. Bulletin of the Seismological Society of America 95 (2), 684–698.

Woessner, J., Hauksson, E., Wiemer, S., Neukomm, S., 2004. The 1997 Kagoshima (Japan) earthquake doublet: a quantitative analysis of aftershock rate changes. Geophysical Research Letters 31, L03605. doi:10.1029/2003GL018858.

Wyss, M., 1973. Towards a physical understanding of the earthquake frequency distribution. Geophysical Journal of the Royal Astronomical Society 31, 341–359.

Wyss, M., Sammis, C.G., Nadeau, R.M., Wiemer, S., 2004. Fractal dimension and b-value on creeping and locked patches of the San-Andreas fault near Parkfield, California. Bulletin of the Seismological Society of America 94, 410–421.

Yadav, R.B.S., 2009. Seismotectonic modeling of NW Himalaya: a perspective on future seismic hazard. Ph.D. Thesis. Department of Earthquake Engineering, IIT Roorkee, India, p. 76.

Yadav, R.B.S., Shanker, D., Singh, V.P., Gupta, S.C., 2005. On the study of seismic activity of Kutch region and aftershock sequences with reference to Bhuj earthquake, 26th January 2001, India. In: Symposium on 'Seismic Hazard Analysis and Microzonation'. Department of Earthquake Engineering, Indian Institute of Technology, Roorkee, India, September 23–24, pp. 119–134.

Yadav, R.B.S., Shanker, D., Chopra, S., Singh, A.P., 2010. An application of regional time and magnitude predictable model for long-term earthquake prediction in the vicinity of October 8, 2005 Kashmir Himalaya earthquake. Natural Hazards 54, 985–1014.

Yadav, R.B.S., Papadimitriou, E.E., Karakostas, V.G., Shanker, D., Rastogi, B.K., Chopra, S., Singh, A.P., Santosh, K., 2011. The 2007 Talala, Saurashtra, western India earthquake sequence: tectonic implications and seismicity triggering. Journal of Asian Earth Sciences 40 (1), 303–314.

Ziv, A., Rubin, A.M., 2000. Static stress transfer and earthquake triggering: no lower threshold in sight? Journal of Geophysical Research 105, 13631–13642.